

Appendix

Supplemental figures and legends

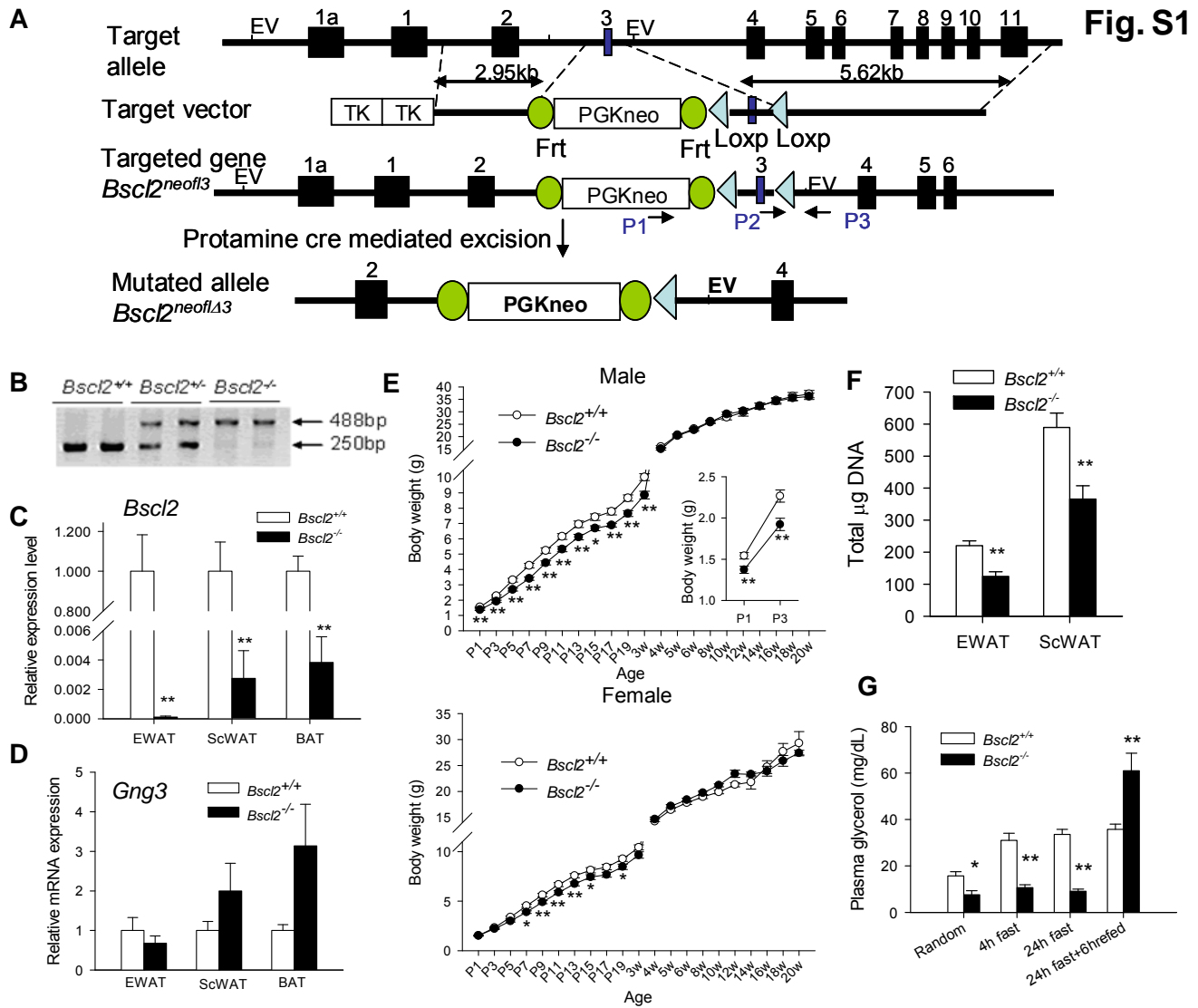


Fig. S1. Generation and characterization of *Bsc12* global deficient mice. (A) Targeting strategy.

The mouse *Bsc12* gene (the target allele) is shown on top with the targeted vector shown below featuring two TK cassettes 5' to the short left homologous arm, followed by the insertion of a PGK-Neo cassette flanked by two Frt sites; the targeted exon 3 and its flanking intronic region was flanked by two loxP sites followed by a long right homologous arm. Deletion of exon 3 will

not only remove a portion of the coding gene, but also lead to a frame-shift mutation generating a premature stop codon one amino acid after the presumed exon skipping. The predicted homologous recombination will generate the *Bscl2*^{neofl3} allele. Global deletion of exon 3 in *Bscl2* gene is achieved by crossing the targeted mice with protamine cre mice as described in supplementary materials and methods, and the predicted mutant allele, *Bscl2*^{neoflΔ3/+}, is shown at the bottom. (B) Genomic PCR genotyping of global heterozygous (*Bscl2*^{neoflΔ3/+}, simplified as *Bscl2*^{+/-}) and homozygous (simplified as *Bscl2*^{-/-}) mice using tail DNA. Three primers (p1, p2 and p3, as indicated in Fig. S1A) are used for genotyping. Primers p1 and p3 amplify the mutant allele of 488bp DNA fragment, while primers p2 and p3 amplify the wild-type allele of 250bp. (C and D) Q-PCR analyses of the mRNA expression of *Bscl2* (C) and its divergently transcribed gene close to *Bscl2*: *Gng3* (D) in epididymal white adipose tissue (EWAT), subcutaneous fat (ScWAT) and brown adipose tissue (BAT). Data were normalized to Cyclophilin A and presented as fold changes compared with the wild-type. (E) Growth curves of male and female *Bscl2*^{+/+} and *Bscl2*^{-/-} mice from postnatal day 1 up to 20 weeks old. *: p < 0.05 between *Bscl2*^{+/+} and *Bscl2*^{-/-} mice (n=15-20 each). (F) Total nuclear DNA contents in the entire EWAT and ScWAT isolated from 8 week old wild-type and *Bscl2*^{-/-} mice (n=7). *, p < 0.05; **, p < 0.005 between wild-type and *Bscl2*^{-/-} mice. (G) Plasma glycerol in 10 week old male wild-type and *Bscl2*^{-/-} mice after random, 4 h fast, 24 h fast and 24 h fast followed by 6 h refed with normal chow diet. *: p < 0.05; **: p < 0.005 vs wild-type under same condition.

Fig S2

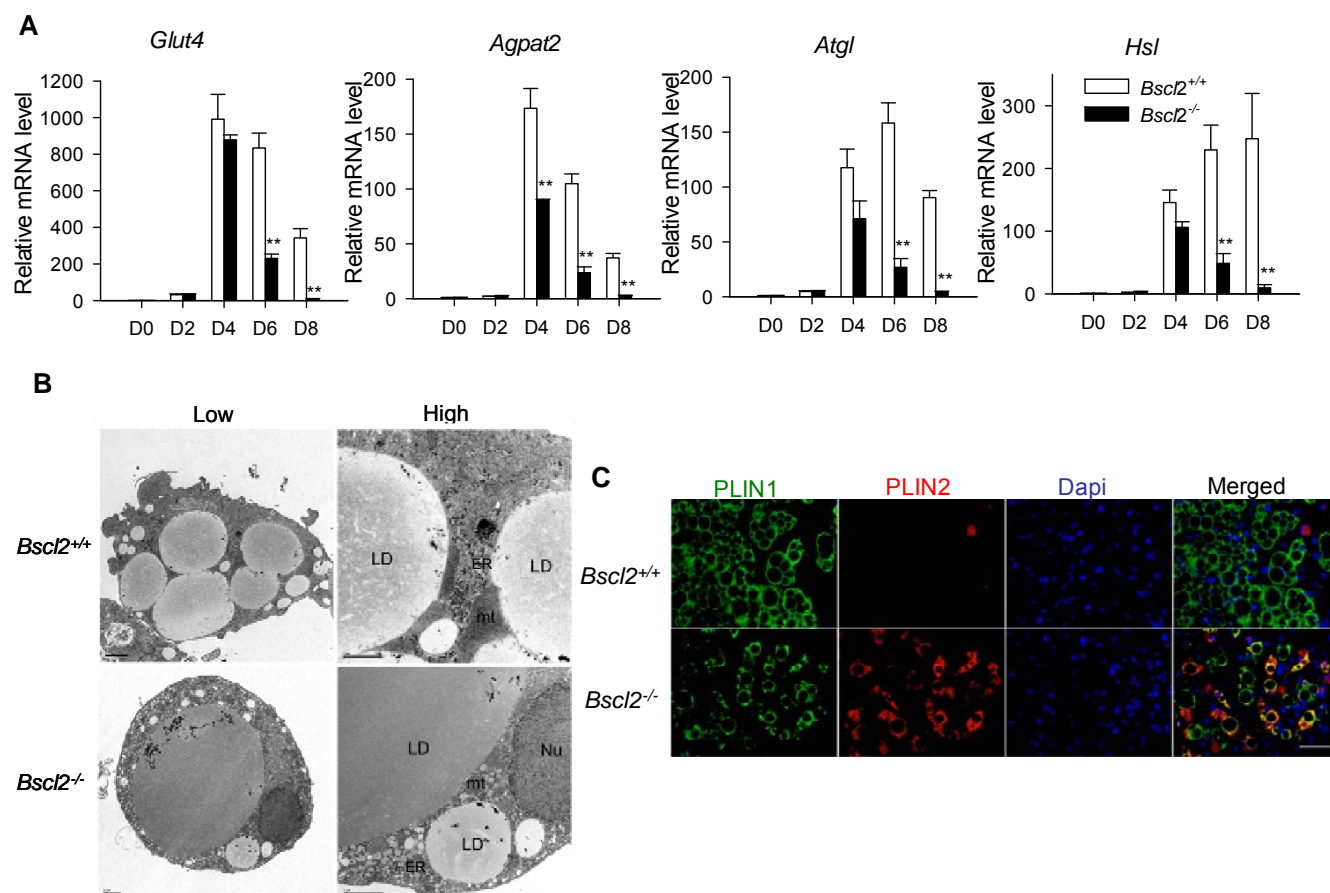


Fig. S2. Molecular characterization of *Bsc12*^{-/-} MEFs undergoing differentiation. (A) Quantitative RT-PCR analyses of *glut4*, *Agpat2*, *Atgl* and *Hsl* in wild-type and *Bsc12*^{-/-} MEFs during adipocyte differentiation. Data were normalized to Cyclophilin A and expressed as relative fold changes as compared to wild-type at D0. *: $p < 0.05$; **: $p < 0.005$ between wild-type and *Bsc12*^{-/-} at the same time point. (B) Conventional Thin-section Electron Microscopy of D6 Differentiating MEF Cells. Lipid droplets (LD) were seen as more or less dense bodies with little internal structure. Mitochondria (mt) were seen as dense subcellular structure apposed to the lipid droplets. Nu, nucleus; ER, Endoplasmic Reticulum. Bars = 2 μm (left), 1 μm (right). (C) Immunofluorescence staining of PLIN1 and PLIN2, two lipid droplet proteins in D6 differentiated wild-type and *Bsc12*^{-/-} MEF cells. FITC conjugated anti-guinea pig secondary antibody was used to label PLIN1 and Rhodamin-conjugated anti-rabbit secondary antibody

was used to label PLIN2 protein. Dapi was used to stain the nuclei. Scale bar = 50 μ m and is applicable to all pictures.

Fig. S3

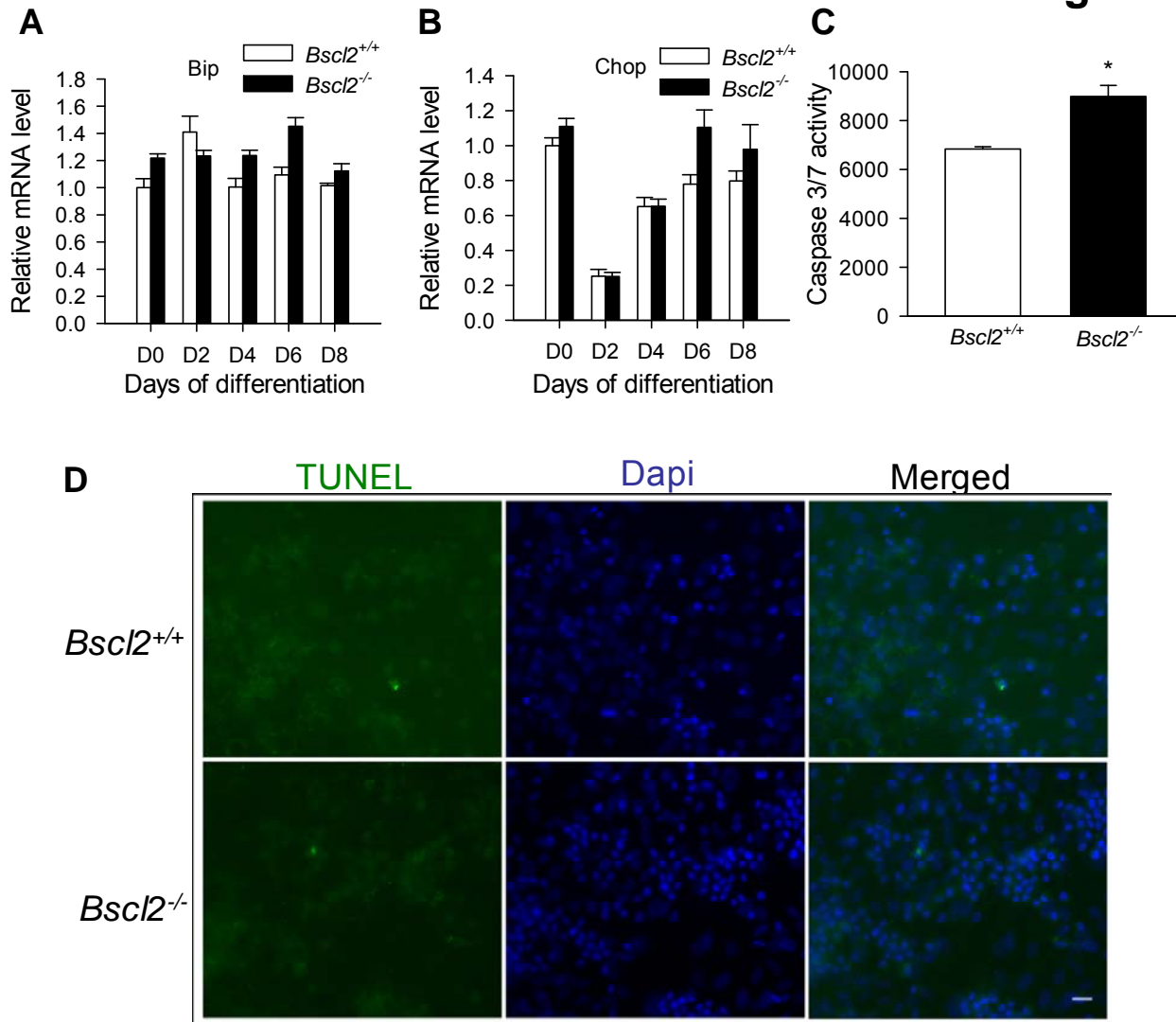


Fig. S3. Apoptosis is not associated with differentiated D10 *Bsc12*^{-/-} MEF cells that were absent of lipid droplet. (A and B) Quantitative RT-PCR analyses of Bip (A) and Chop (B) in wild-type and *Bsc12*^{-/-} MEFs undergoing differentiation. (C) Caspase 3/7 activity assay performed in D10 wild-type and *Bsc12*^{-/-} MEFs. The results are average of 6 duplicates and repeated from three independent experiments. (D) TUNEL staining on D10 differentiated wild-type and *Bsc12*^{-/-} MEF adipocytes. The few TUNEL positive (green fluorescence) signals that overlapped with nuclear Dapi staining indicate apoptotic cells. Scale bar = 50 μ m and applies to each picture.

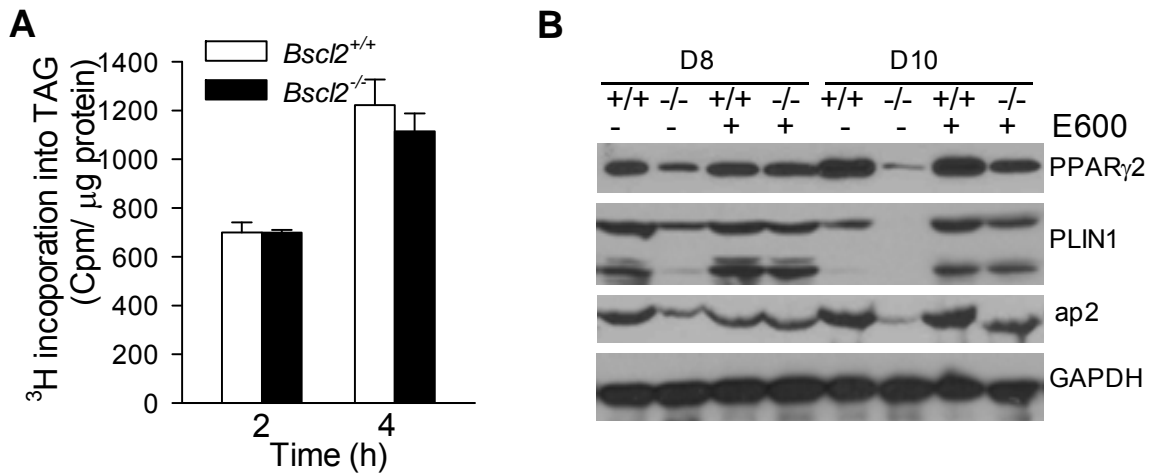
Fig. S4

Fig. S4. TAG synthesis and protein expression in differentiating wild-type and *Bsc12*^{-/-} MEFs. (A) *In vitro* TAG synthesis rate in D4 differentiating wild-type and *Bsc12*^{-/-} MEFs. The incorporation rate of [³H] oleate into TAG was normalized to cellular protein content. (B) Western blot analyses of mature adipocyte markers in differentiated wild-type (+/+) and *Bsc12*^{-/-} (-/-) MEFs harvested at indicated days with (+) or without (-) E600 treatment. Same amounts of proteins were loaded and GAPDH was used as loading control.

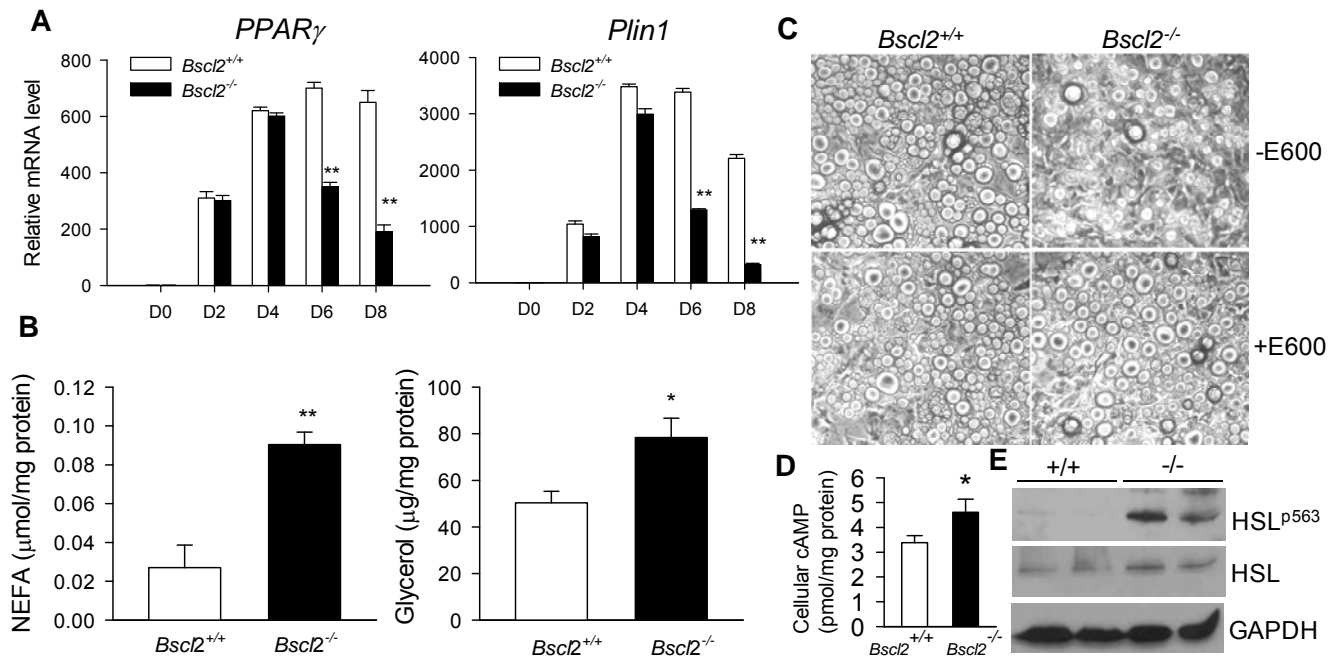
Fig. S5

Fig. S5. Differentiation from *Bsc12^{-/-}* stromal vascular cells (SVCs) essentially repeats the same findings as *Bsc12^{-/-}* MEF cells. (A) qPCR analysis of *PPAR γ* and *Plin1* in wild-type and *Bsc12^{-/-}* SVCs undergoing differentiation. Data were normalized to Cyclophilin A and expressed as relative fold change as compared to wild-type at D0. *, p < 0.05; **, p < 0.005 vs. wild-type on the same day. (B) NEFA and glycerol release in D4 differentiating wild-type and *Bsc12^{-/-}* SVCs under basal condition *in vitro*. *, p < 0.05; **, p < 0.005. (C) Microscopic analysis of induced adipose differentiation in wild-type and *Bsc12^{-/-}* SVCs at D10 after induction with (+E600) or without (-E600) lipase inhibitor E600 treatment from D4 *in vitro*. (D) Cellular cAMP contents in D4 differentiating wild-type and *Bsc12^{-/-}* SVC cells. (E) Western blot analysis of lipolysis-related proteins in D4 *Bsc12^{+/+}* (+/+) and *Bsc12^{-/-}* (-/-) SVC whole cell lysates.

Supplemental materials and methods

Generation of global *Bsc12* deficient mice. The targeting construct contains two thymidine kinase (TK) cassettes for negative selection and a neomycin cassette (Neo) for positive selection which is flanked by two Frt sites for removal of the Neo by FLP recombinase. The targeted exon 3 with its flanking intronic regions was flanked by two loxP sites (Supplementary Fig. 1A). The construct was introduced into mouse R1 ES cells by electroporation. Two independent recombinant ES cell clones were injected into C57BL/6J blastocysts and 4 chimeric founders were obtained. The chimeric founder mice were crossed to C57BL/6J mice and agouti offspring were genotyped. We call the mice that contain both Neo and floxed site in one *Bsc12* allele as the *Bsc12*^{neof13/+} mice.

To generate animals with whole-body excision of the floxed exon, the *Bsc12*^{neof13/+} mice were crossed to a line expressing Cre recombinase in the testis (*Protamine-Cre*, C57BL/6J genetic background). Male *Bsc12*^{neof13/+} offsprings with a *Protamine-Cre* transgene were bred to C57BL/6J, and their offsprings were assessed as the heterozygous mice with a deletion of exon 3. Subsequently, the *Protamine-Cre* negative heterozygous mice (F4) were mated to generate wild-type and homozygous *Bsc12*^{-/-} littermates for studies.

Measurement of triacylglycerol synthesis. D4 differentiating MEF cells were incubated with 400 μ M oleic acid (containing 1 μ Ci [³H] oleate /60-mm culture dish) bound to fatty acid-free BSA at a molar ration of 6:1 in the presence of TAG hydrolyase inhibitor E600 as previously described (1). After indicated time, we removed the media, washed the cells twice with PBS, and extracted lipids for thin layer chromatography analysis. Incorporation of radioactive oleate into triacylglycerols was determined by liquid scintillation counting of the corresponding silica gel bands that contain triacylglycerols. The [³H] oleate incorporation rate was normalized to cellular protein content.

Electron microscopy. Samples of D6 differentiated MEFs were fixed with 2.5% glutaraldehyde/0.1M cacodylate and lead citrate. The ultra thin sections were examined under a Hitachi H-7500 Transmission Electron Microscope (TEM).

Assay for caspase-3/7 activity. Caspase 3/7 activity in D10 differentiated wild-type and *Bsc12*^{-/-} MEF cells were measured by using high sensitive Caspase-GloTM 3/7 assay kit (promega) according to the manufacturer's instruction. Briefly, cells were trypsinized and counted. Each reaction contains 10⁶ cells in 100 µl media and mixed with 100 µl caspase 3/7 assay reagent. After 1 h incubation at room temperature, luminance was read at LUMIstar OPTIMA luminometer (BMG Lab Tech Co.).

TUNEL staining to detect apoptosis. D10 differentiated wild-type and *Bsc12*^{-/-} MEF cells were fixed in 4% paraformaldehyde. Apoptotic cells were detected by using In situ cell death detection fluorescein kit (Roche applied Sciences) according to the manufacturer's instruction. Fluorescence was imaged under a Zeiss Axioplan-2 Imaging System.

Supplemental references

1. **Brasaemle, D. L., B. Rubin, I. A. Harten, J. Gruia-Gray, A. R. Kimmel, and C. Londos.** 2000. Perilipin A increases triacylglycerol storage by decreasing the rate of triacylglycerol hydrolysis. *J Biol Chem* **275**:38486-93.